

Morphometric Examination of Mitochondrial Ultrastructure in Aging Cardiomyocytes

Ch. M. El'darov^{1,2}, V. B. Vays^{1,2}, I. M. Vangeli^{1,2}, N. G. Kolosova³, and L. E. Bakeeva^{1,2*}

¹*Lomonosov Moscow State University, Belozersky Institute of Physico-Chemical Biology, 119991 Moscow, Russia; fax: +7 (495) 939-3181; E-mail: fhb@belozersky.msu.ru; bakeeva@belozersky.msu.ru*

²*Lomonosov Moscow State University, Institute of Mitoengineering, 119991 Moscow, Russia; fax: +7 (495) 939-5945; E-mail: info@mitotech.ru*

³*Institute of Cytology and Genetics, Siberian Branch of the Russian Academy of Sciences, 630090 Novosibirsk, Russia; fax: +7 (383) 333-1278; E-mail: kolosova@bionet.nsc.ru*

Received December 17, 2014

Revision received January 28, 2015

Abstract—Mitochondrial ultrastructure in cardiomyocytes from 3- and 24-month-old Wistar and OXYS rats was investigated using a new approach designed for morphometric analysis. The data fully confirm the electron microscopy data: the area of the inner mitochondrial membrane per unit volume of mitochondria was significantly decreased with age, as found on heart muscle section. In 3-month-old Wistar rats from the control group, this parameter was $41.3 \pm 1.52 \mu\text{m}^2/\mu\text{m}^3$, whereas in OXYS rats it was decreased to $30.57 \pm 1.74 \mu\text{m}^2/\mu\text{m}^3$. With age, an area of the inner mitochondrial membrane per unit volume of mitochondria declined in both rat strains: Wistar – from 41.3 ± 1.52 to $21.47 \pm 1.22 \mu\text{m}^2/\mu\text{m}^3$, OXYS – from 30.57 ± 1.74 to $16.3 \pm 0.89 \mu\text{m}^2/\mu\text{m}^3$. A new method that we designed and used for morphometric analysis notably simplifies the process of morphometric measurements and opens up good opportunities for its further optimization using image recognition technology.

DOI: 10.1134/S0006297915050132

Key words: morphometry, aging, ultrastructure, cardiomyocyte

Currently, more attention is given to the studies investigating age-related processes including age-dependent changes in organs and body tissues. Examination of age-related changes in myocardium represents one of the lead directions in this area, as heart diseases are among the major causes of mortality in the human population. According to the World Health Organization, every year the proportion of cardiovascular diseases among age-related pathologies increases [1].

Based on the free radical theory proposed by Harman [2], a mitochondrial theory of aging was formulated that was further extended by V. P. Skulachev. According to this theory, changes in functional state of mitochondria resulting in excessive generation of reactive oxygen species (ROS) is the main factor in development of the age-related changes in organs and body tissues [3-7]. Oxidative stress caused by ROS plays a central role in normal physiological aging and etiology of many serious myocardial pathologies [8-15]. The functional state of mitochondria is well known to be related to changes in

their ultrastructure [16-20]. Therefore, investigation of the age-related morphological changes in mitochondria is a very promising direction, as alterations in mitochondrial ultrastructure occur much before clinical symptoms of disease are manifested. At the same time, specific features of the mitochondrial ultrastructure point to changes in functional state of the body tissue and, consequently, the onset of developing pathology.

Not only a qualitative, but also a quantitative evaluation of the obtained data by morphometric and stereological analysis of mitochondrial ultrastructure play an important role while examining mitochondrial ultrastructure. During such studies, a common approach is to measure length and width of the mitochondria as well as total and mean cross-sectional area, mitochondrial volume fraction per section, and area of the inner mitochondrial membrane per unit volume of mitochondria [21, 22]. A common method is based on using the sets of points, lines, concentric arcs and circles overlapped over an image followed by counting the number of points fitting within the structures or a number of test line intersections [23-25]. Such methods require a high labor input

* To whom correspondence should be addressed.

and a large number of measurements as well as time consumed for calculations. Using computer software to analyze electron microscopy data such as image recognition and processing can simplify and to lower a number of measurements necessary to evaluate morphometric parameters of mitochondria, particularly, area of the inner mitochondrial membrane per unit volume of mitochondria as one of the most important morphometric parameters that allows assessment of the functional state of mitochondria. Using graph software suites opens up an opportunity for further automation of the analysis of electron microscopy images.

The current study was aimed at applying a new method that we proposed for morphometric analysis of mitochondria both in automated and semi-automated mode to assess results of electron microscopy examination. This method was used for morphometric processing of the aging-related ultrastructural changes in cardiomyocyte mitochondria isolated from Wistar and OXYS rat strains. Interestingly, OXYS rat strain represents a unique model for examining the role of oxidative stress in development of age-related pathologies. Rats of this strain are characterized by early involutive changes in internal organs and impaired functioning of the central nervous system typical for other aging animals and human. An enhanced generation of oxygen radicals detected in body tissues is a key characteristic of the OXYS rat strain [26].

MATERIALS AND METHODS

Animals. A model a premature aging was developed at the Institute of Cytology and Genetics, Siberian Branch of the Russian Academy of Sciences, using the OXYS rat strain inbred with Wistar rats most susceptible to cataractogenic effect of galactose diet [27, 28]. The final rat strain was registered at the Rat Genome international database (<http://rgd.mcw.edu>). To date, there has been obtained 99 generations of the OXYS rat strain having the syndrome of accelerated aging.

For experiments, 24-month-old male Wistar ($n = 15$) and OXYS ($n = 15$) rats were used. They were obtained from the Center for Collective Use "Gene Bank of Experimental Animals", Institute of Cytology and Genetics, Siberian Branch of the Russian Academy of Sciences. The animals were housed in groups of five per cage, natural illumination, air temperature $22 \pm 2^\circ\text{C}$, and free access to water and feed (RK-120-1; Laboratornab, Russia). In control group, 3-month-old Wistar ($n = 5$) and OXYS ($n = 5$) rats were used to assess age-related changes in myocardial tissues.

All procedures were performed according to the European Union Council Directive 86/609/EEC.

Electron microscopy. For this examination, tissue of the left ventricular wall was excised followed by fixation in 3% glutaraldehyde in phosphate buffer (pH 7.4) for 2 h,

4°C , and further fixation in 1% osmium tetroxide buffer for 1.5 h, and dehydration in solutions with ascending alcohol concentrations (70% alcohol solution was saturated by uranyl acetate). After that, tissue was embedded in Epon-812 epoxy resin. Serial ultrathin sections were made using a Leica ultramicrotome (Germany) followed by lead staining according to Reynolds. The data were viewed and photographed using an H-12 electron microscope (Hitachi, Japan). Final images were scanned at 1200 and 2400 dpi resolution.

Morphometry and statistical analysis. For morphometric examination, 50 electron microscopy images of myocardial tissue from each group were selected. Each image was scanned at a preset resolution (dpi) allowing calculation of its scale, i.e. number of pixels per unit of actual length (1 nm), according to the formula:

$$K_{\text{pix/nm}} = M \cdot R_s / 25.4 \cdot 10^6, \quad (1)$$

where M – magnification of a microscope, R_s – scan resolution.

Single mitochondria were outlined manually on each image followed by delineating their inner membranes (Fig. 1, a-c). Width of line used to delineate inner membranes was picked according to the k magnitude (pixel/nm) calculated according to formula (1) by taking the mean width of the inner mitochondrial membrane on image equal to 75 \AA (Fig. 1, a-c). By taking into consideration the scale of image as well as the known section thickness $\sim 700 \text{ \AA}$, various morphometric parameters such as an area of the inner mitochondrial membrane inside section volume, total length of the inner mitochondrial membrane, and volume of mitochondria inside section were calculated using Adobe Photoshop suite software (Adobe Systems, Inc., USA). Herein, it was assumed that the membranes of interest were located strictly perpendicularly towards a section plane, whereas non-perpendicular membranes would not be seen on the image, which gave an error not exceeding 4%. From the data, area of the inner mitochondrial membrane (μm^2) per unit of volume of mitochondria (μm^3) was calculated. Statistical processing of the morphometric data was performed by using STATISTICA 8 software suite (StatSoft Inc., USA). Significance level was checked using the Mann–Whitney test.

RESULTS

A typical picture of the mitochondrial ultrastructure in cardiomyocytes from 3-month-old Wistar rats is presented in Fig. 2a. It was found that the mitochondrial ultrastructure corresponded to the functionally active orthodox state according to the classification by Green [29]. The inner mitochondrial membrane formed multiple cristae deviating by dense parallel rows into the organelle and filling up the entire internal space of the

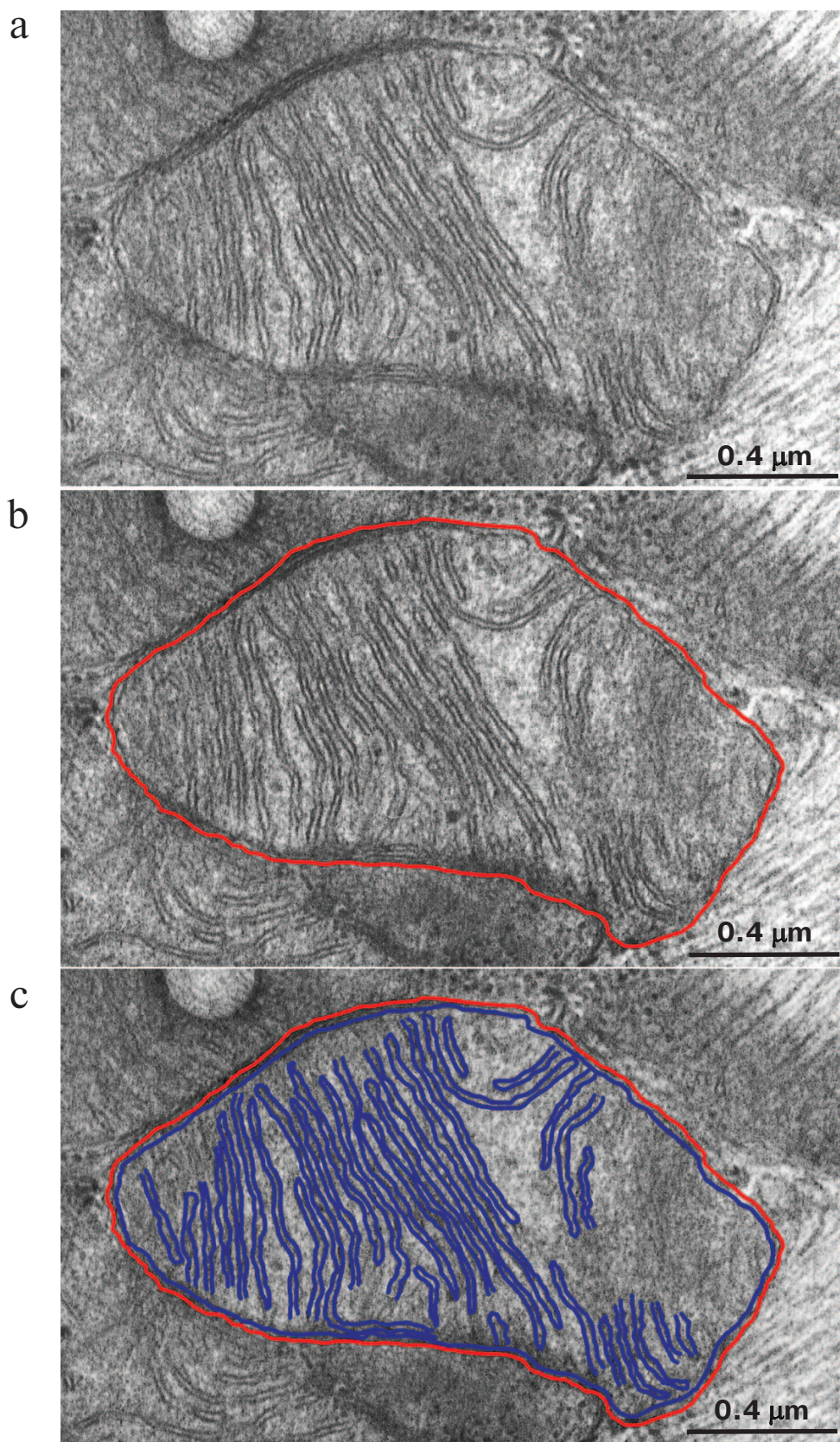


Fig. 1. Method used for isolation of mitochondrial membranes is depicted using Adobe Photoshop. a) Baseline electron microscopy image of mitochondria in 3-month-old OXYS rats; b) the outer mitochondrial membrane is highlighted in red; c) the inner mitochondrial membrane is highlighted in blue.

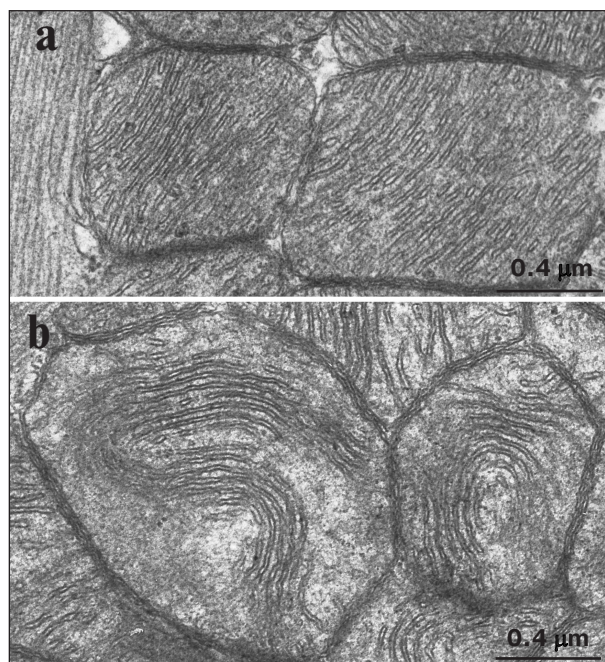


Fig. 2. Ultrastructure of cardiomyocyte mitochondria in Wistar rats: a) 3-month-old; b) 24-month-old.

mitochondria. The matrix of mitochondria was prominent, whereas the inter-membrane space (narrow lumens inside the cristae and between the inner and outer mitochondrial membranes) was electron light. A picture of the mitochondrial ultrastructure typical of cardiomyocytes from 24-month-old Wistar rats is shown in Fig. 2b. It is clear that internal mitochondrial ultrastructure in Wistar rats starts to change significantly with age. In particular, the number of mitochondrial cristae was markedly reduced, they started to lose strict parallel position, and they did not fill the entire internal space of the mitochondria, thus resulting in the appearance of electron light areas inside the mitochondrial matrix. Also, it is shown that some cristae, being still mutually parallel, started to form a bending chord freely positioned inside the electron light matrix.

Morphometric analysis of 50 electron microscopy images of cardiomyocytes from each animal group was performed to evaluate mitochondrial ultrastructure as well as to determine if the observed age-related changes in mitochondrial ultrastructure have a single pattern. The results of measuring surface area of the inner mitochondrial membrane per unit volume of mitochondria in Wistar rats are shown in Fig. 3. It was found that at the age of 3 months it reached $41.3 \pm 1.52 \mu\text{m}^2/\mu\text{m}^3$, whereas at age of 24 months this parameter was significantly decreased 2-fold to $21.47 \pm 1.22 \mu\text{m}^2/\mu\text{m}^3$.

A typical cardiomyocyte mitochondrial ultrastructure found in 3-month-old OXYS rats is shown in Fig. 4a. Note that as early as at age of 3 months, the OXYS rats started to

accumulate destructive changes in their mitochondria manifested as the first signs of disturbed internal organization. Some parts of the organelle contain cristae that started to lose dense mutually parallel position, with appearance of electron-light areas. Interestingly, mitochondrial ultrastructure in 3-month-old OXYS rats was similarly altered as in 24-month-old Wistar rats. An electron microscopy image of mitochondria from myocardial tissue of 24-month-old OXYS rats is shown in Fig. 4b. Profound disturbances in the internal ultrastructure of the mitochondria are evident. The inner mitochondrial membrane forms scarce cristae that preserve their order only at some sites in the mitochondria. A marked translucency of mitochondrial matrix is observed. A major part of the mitochondrial matrix is filled with electron-light areas.

In addition, an area of the inner mitochondrial membrane per unit volume of mitochondria was calculated for OXYS rats while analyzing morphometric data of electron microscopy images (Fig. 3). Even at age of 3 months, this parameter was substantially lower in OXYS vs. Wistar rats (30.57 ± 1.74 vs. $41.3 \pm 1.52 \mu\text{m}^2/\mu\text{m}^3$, respectively). By 24 months, mean area of the inner mitochondrial membrane per unit volume of mitochondria in OXYS rats also dropped by ~ 2 -fold similar to Wistar rats (from 30.57 ± 1.74 to $16.3 \pm 0.89 \mu\text{m}^2/\mu\text{m}^3$).

DISCUSSION

The results of our study indicate that the proposed method of morphometric analysis for evaluating mitochondrial ultrastructure is highly productive. The morphometric analysis of the data not only fully proves but also supplements electron microscopy observations unveiling a pattern of changes in cardiomyocyte ultra-

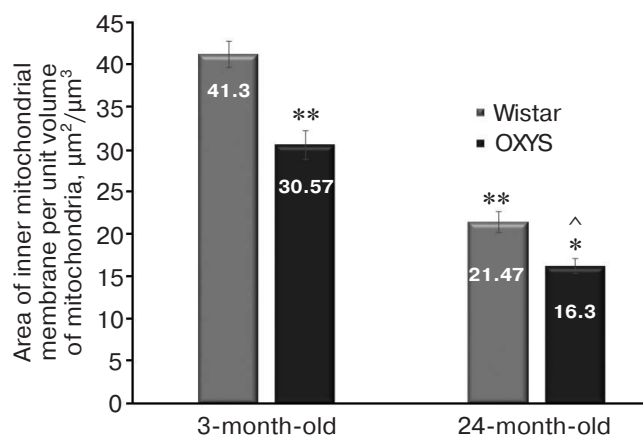


Fig. 3. Mean area of the inner mitochondrial membrane per unit volume of mitochondria in cardiomyocytes from Wistar and OXYS rats upon aging; * $p < 0.01$ vs. 3-month-old OXYS rats; ** $p < 0.01$ vs. 3-month-old Wistar rats; ^ $p < 0.01$ vs. 24-month-old Wistar rats. Error bars correspond to standard error of mean.

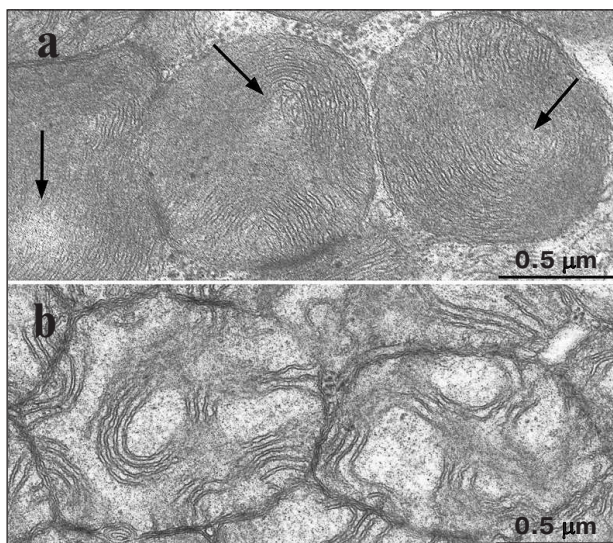


Fig. 4. Internal ultrastructure of mitochondria in cardiomyocytes from OXYS rats: a) 3-month-old, arrows depict electron-light areas; b) 24-month-old.

structure of mitochondria found upon aging. The data about the magnitude of an area of the inner mitochondrial membrane per unit volume of mitochondria were found to fully agree with the data of visual observations, thus allowing evaluation of the degree of ultrastructural alterations in the mitochondria. In particular, a significant age-related reduction of this morphometric parameter in both Wistar and OXYS rats was observed (Fig. 3) that may evidence dysfunction of mitochondria and the myocardium as a whole. Whereas in 3-month-old Wistar rats from control group, it was $41.3 \pm 1.52 \mu\text{m}^2/\mu\text{m}^3$, in OXYS rats of the same age the area of the inner mitochondrial membrane per unit volume of mitochondria was reduced by almost 25% and comprised $30.57 \pm 1.74 \mu\text{m}^2/\mu\text{m}^3$. It should be noted that these parameters in both groups were reduced in approximately the same way, 2-fold compared to the baseline: Wistar rats – from 41.3 ± 1.52 to $21.47 \pm 1.22 \mu\text{m}^2/\mu\text{m}^3$, OXYS rats – from 30.57 ± 1.74 to $16.3 \pm 0.89 \mu\text{m}^2/\mu\text{m}^3$. However, area of the inner mitochondrial membrane per unit volume of cardiomyocyte mitochondria was significantly reduced in OXYS rats compared to Wistar rats from control group (16.3 ± 0.89 vs. $21.47 \pm 1.22 \mu\text{m}^2/\mu\text{m}^3$, respectively). Thus, akin to the data of visual observations, morphometric analysis of the mitochondrial ultrastructure demonstrated that the age-related changes in mitochondrial ultrastructure in cardiomyocytes develop much earlier in OXYS rats compared to control Wistar rats and deteriorate with age.

In most cases, a point-count system proposed by A. A. Glagolev [30] and later described by Weibel [23] has been used to measure different morphometric parameters of cells and body tissues. Percentage of points fitting the structure profile as well as a number of intersections with

test lines determine relative volume, area, mean length, width of organelles, and other parameters. In particular, this approach was applied for examining myocardium in Syrian hamsters upon aging [31]: it was demonstrated that a marked age-related decrease in the volume of sarcoplasmic reticulum paralleled simultaneous elevation of the fat drop count. In addition, mean area of the inner mitochondrial membrane per unit volume of mitochondria was decreased. Frenzel and Feimann found that the mitochondrial volume fraction both in the left and right ventricles were decreased in 2-year-old vs. 6-week-old Wistar rats from control group. Mean size of mitochondria was decreased by 36 and 11% for the left and right ventricles, respectively [32].

Other methods including a manual calculation of structure profiles using electron microscopy images as well as analysis of images performed by using a specially designed computer software were also used for morphometry of cardiomyocytes. These methods were also based on a basic method of counting points and lines [33, 34]. Often, all the aforementioned methods require development of special test systems most perfectly fitting to the specifics of the particular study. Perhaps, this may explain the fact that attention in such studies is mainly given to evaluating condition of entire body tissue or dynamic changes in the number of myofibrils, whereas morphometry of the internal organization of cardiomyocyte mitochondria remains poorly investigated as the point-and-line system manually used for analysis of the internal organization of mitochondria cannot provide a precise, objective, and statistically significant evaluation of the mitochondrial ultrastructure. We attempted to fully abandon using the generally accepted application of point-and-line system. The results of preliminary studies obtained during development of the proposed method revealed that it was effective [35]. The method used in the current study significantly simplifies morphometric measurements and opens up good opportunities for its further optimization by using image recognition technology. In our opinion, application of morphometric methods together with histology and biochemical methods is considered highly perspective in not only finding and understanding correlations between parameters of mitochondrial ultrastructure and their functional state but also for evaluating functional status of the body tissue as a whole.

This study was conducted with the financial support from the Russian Science Foundation (project No. 14-50-00029).

REFERENCES

1. *Ten Prominent Causes of Mortality Worldwide* (2014) World Health Organization, News Bulletin No. 310 (<http://www.who.int/mediacentre/factsheets/fs310/en/>).

2. Harman, D. (1956) Aging: a theory based on free radical and radiation chemistry, *J. Gerontol.*, **11**, 298-300.
3. Harman, D. (1972) The biologic clock: the mitochondria, *J. Am. Geriatr. Soc.*, **20**, 145-147.
4. Miquel, J., Economos, A. C., Fleming, J., and Johnson, J. E. (1980) Mitochondrial role in cell aging, *Exp. Gerontol.*, **15**, 575-591.
5. Skulachev, V. P. (1997) Body aging – a special biological function rather than a result of a complicated biological system failure: a biological justification for Weismann's hypothesis, *Biochemistry (Moscow)*, **62**, 1191-1195.
6. Skulachev, V. P. (1999) Phenoptosis: a programmed body death, *Biochemistry (Moscow)*, **64**, 1418-1426.
7. Skulachev, V. P. (2001) Events of the programmed death. Mitochondria, cells and organs: a role for reactive oxygen intermediates, *Soros. Obrazovat. Zh.*, **7**, 4-10.
8. Lenaz, G. (2001) The mitochondrial production of reactive oxygen species: mechanisms and implications in human pathology, *IUBMB Life*, **52**, 159-164.
9. Andreev, A. Yu., Kushnareva, Yu. E., and Starkov, A. A. (2005) A metabolism of reactive oxygen intermediates in mitochondria, *Biochemistry (Moscow)*, **70**, 200-214.
10. Honda, H. M., Korge, P., and Weiss, J. N. (2005) Mitochondria and ischemia/reperfusion injury, *Ann. N. Y. Acad. Sci.*, **1047**, 248-258.
11. Zweier, J. L., and Talukder, M. A. (2006) The role of oxidants and free radicals in reperfusion injury, *Cardiovasc. Res.*, **70**, 181-190.
12. Yellon, D. M., and Hausenloy, D. J. (2007) Myocardial reperfusion injury, *N. Engl. J. Med.*, **357**, 1121-1135.
13. Eltzschig, H. K., and Eckle, T. (2011) Ischemia and reperfusion – from mechanism to translation, *Nature Med.*, **17**, 1391-1401.
14. Borutaite, V., Toleikis, A., and Brown, G. C. (2013) In the eye of the storm: mitochondrial damage during heart and brain ischaemia, *FEBS J.*, **280**, 4999-5014.
15. Chouchani, E. T., Pell, V. R., Gaude, E., Aksentijevic, D., Sundier, S. Y., Robb, E. L., Logan, A., Nadtochiy, S. M., Ord, E. N., Smith, A. C., Eyassu, F., Shirley, R., Hu, C. H., Dare, A. J., James, A. M., Rogatti, S., Hartley, R. C., Eaton, S., Costa, A. S., Brookes, P. S., Davidson, S. M., Duchon, M. R., Saeb-Parsy, K., Shattock, M. J., Robinson, A. J., Work, L. M., Frezza, C., Krieg, T., and Murphy, M. P. (2014) Ischaemic accumulation of succinate controls reperfusion injury through mitochondrial ROS, *Nature*, **515**, 431-435.
16. Hackenbrock, C. R. (1966) Ultrastructural bases for metabolically linked mechanical activity in mitochondria. I. Reversible ultrastructural changes with change in metabolic steady state in isolated liver mitochondria, *J. Cell Biol.*, **30**, 269-297.
17. Hackenbrock, C. R. (1968) Chemical and physical fixation of isolated mitochondria in low-energy and high-energy states, *Proc. Natl. Acad. Sci. USA*, **61**, 598-605.
18. Green, D. E., Asai, J., and Harris, R. A. (1968) Conformational basis of energy transformations in membrane systems. III. Configurational changes in the mitochondrial inner membrane induced by changes in functional states, *Arch. Biochem. Biophys.*, **125**, 684-705.
19. Bakeeva, L. E., Severina, I. I., Skulachev, V. P., Chentsov, Yu. S., and Yasaytis, A. A. (1971) Penetrating ions and structure of mitochondria, in *Mitochondria. Structure and Functions in Health and Pathology* [in Russian], Nauka, Moscow.
20. Bakeeva, L. E., and Yasaytis, A. A. (1972) Changes in structure of mitochondria in response to functional impacts, in *Mitochondria. Molecular Mechanisms of Enzymatic Reactions* [in Russian], Nauka, Moscow, pp. 56-64.
21. McCallister, B. D., and Brown, A. L. (1965) A quantitative morphological study of the mitochondria in experimental cardiac hypertrophy, *Lab. Invest.*, **14**, 692-700.
22. Cieciora, L., Rydzynski, K., and Klitonczyk, W. (1979) Stereologic studies on mitochondrial configuration in different organs of the rat, *Cell Tissue Res.*, **196**, 347-360.
23. Weibel, E. R. (1979) *Stereological Methods*. Vol. 1. *Practical Methods for Biological Morphometry*, Academic Press, London.
24. Gundersen, H. J., Bendtsen, T. F., Korbo, L., Marcussen, N., Moller, A., Nielsen, K., Nyengaard, J. R., Pakkenberg, B., Sorensen, F. B., and Vesterby, A. (1989) Some new, simple and efficient stereological methods and their use in pathological research and diagnosis, *APMIS*, **96**, 379-394.
25. Mandarim-de-Lacerda, C. A. (2003) Stereological tools in biomedical research, *An. Acad. Bras. Cienc.*, **75**, 469-486.
26. Zhdankina, A. A., Fursova, A. Z., Logvinov, S. V., and Kolosova, N. G. (2008) Clinical and morphological characteristics of chorio-retinal degeneration in early aging OXYS rats, *Bull. Exp. Biol. Med.*, **146**, 455-458.
27. Solov'eva, N. A., Morozkova, T. S., and Salganik, R. I. (1975) Breeding of rat substrain with signs of hereditary galactosemia and examination of their biochemical features, *Genetika*, **18**, 63-71.
28. Rummyantseva, Yu. V., Fursova, A. Zh., Fedoseeva, L. A., and Kolosova, N. G. (2008) Alteration of physico-chemical characteristics and α -crystallin gene expression in lenses of OXYS rats during cataract development, *Biochemistry (Moscow)*, **73**, 1176-1182.
29. Green, D. E., and Baum, H. (1970) *Energy and the Mitochondrion*, Academic Press, N. Y.-London.
30. Glagolev, A. A. (1941) *Geometric Methods of Quantitative Aggregate Analysis by Using Microscope* [in Russian], Gosgeolizdat, Moscow.
31. Sachs, H. G., Colgan, J. A., and Lazarus, M. L. (1977) Ultrastructure of the aging myocardium: a morphometric approach, *Am. J. Anat.*, **150**, 63-71.
32. Frenzel, H., and Feimann, J. (1984) Age-dependent structural changes in the myocardium of rats. A quantitative light- and electron-microscopic study on the right and left chamber wall, *Mech. Ageing Dev.*, **27**, 29-41.
33. Zacharova, G., and Kubinova, L. (1995) Stereological methods based on point counting and unbiased counting frames for two-dimensional measurements in muscles: comparison with manual and image analysis methods, *J. Muscle Res. Cell Motil.*, **16**, 295-302.
34. Tang, Y., Nyengaard, J. R., Andersen, J. B., Baandrup, U., and Gundersen, H. J. (2009) The application of stereological methods for estimating structural parameters in the human heart, *Anat. Rec. (Hoboken)*, **292**, 1630-1647.
35. Pilipenko, D. I. (2010) *Morphometric-Stereological Analysis of Mitochondrial Ultrastructure during Oxidative Stress: synopsis of candidate dissertation* [in Russian], MGU, Moscow.